The optimal and near-optimal wavepacket in a boundary layer and its ensuing turbulent spot

Stefania CHERUBINI [1,2], Jean-Christophe ROBINET[2], Alessandro BOTTARO[3], Pietro DE PALMA[1]

[1]Politecnico of Bari, Italy [2]Arts et Metiers ParisTech, France [3]University of Genova, Italy

LadHyX, 3 December 2009

Outline

1. Motivation
2. Numerical tools and methods
   - Timestepping code
   - Direct-adjoint optimization method
   - Global instability model optimization
3. Linear results
   - The global optimal perturbation
   - Analysis of the streamwise modulation
   - Analysis of the spanwise modulation
   - The global near-optimal perturbation
4. Non linear results
   - Transition energy levels
   - Mechanism of transition
5. Conclusions

Motivation

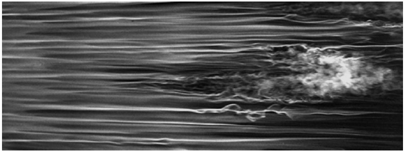

Figure: Wind tunnel smoke visualization of transition in a boundary layer subjected to free stream turbulence (KTH, Stockholm).

- **Emmons (1951): Observation of turbulence spots** → which perturbation most easily bring the flow to turbulent transition?
- **Farrell (1988): Optimal single-wavenumber perturbations** → introduced to explain the occurrence of bypass transition.
- **Biau, Soueid & Bottaro (2008) : Direct numerical simulations** → suboptimal disturbances are more efficient than optimal ones.
- **This work: Optimization of a spatially localized wave packet** → not the traditional inflow-outflow problem, but a new attempt to identify initial localized disturbances that yield convected turbulent spots.

Optimization of a localized wave packet

From single-wavenumber to multiple-wavenumber optimization:

- **Local optimization**: optimization on a velocity profile by direct-adjoint iterations of the Orr-Sommerfeld and Squire equations (Corbett & Bottaro, 2000), the perturbation is characterized by a single wave number in x and z:

$$\mathbf{q}(x,y,z,t)=\tilde{\mathbf{q}}(y,t)\text{exp}\left(i(\beta z+\alpha x)\right) \tag{1}$$

- **Global 2D optimization**: optimization on top of a 2D velocity field by a global eigenvalue model (Alizard & Robinet, 2007), the perturbation is characterized by a single wave number in z:

$$\mathbf{q}(x,y,z,t)=\hat{\mathbf{q}}(x,y,t)exp\left(i\beta z\right) \tag{2}$$

- **Global three-dimensional optimization**: optimization on top of a 2D velocity field by direct-adjoint iterations of the linearized Navier–Stokes equations, the perturbation has no fixed wave number $\rightarrow$ **optimal wave packet localized in the streamwise direction.**

Timestepping code

Non-dimensional incompressible Navier–Stokes equations:

$$\begin{aligned} \mathbf{u}_t + (\mathbf{u} \cdot \bigtriangledown)\mathbf{u} &= -\bigtriangledown p + \frac{1}{Re} \bigtriangledown^2 \mathbf{u}, \\ \bigtriangledown \cdot \mathbf{u} &= 0, \end{aligned} \tag{3}$$

with $\mathbf{u} = (u, v, w)^T$ the velocity vector, p the pressure and $Re = \frac{U_\infty \delta^*}{\nu}$

- '*Fractional step*' method on a '*staggered*' grid.
- Centered second-order spatial discretization
- Temporal discretization: Crank–Nicolson for the viscous terms, third-order Runge-Kutta for non-linear ones.
- Domain: $400 \times 20 \times 10$ in terms of δ_1, discretized on a $501 \times 150 \times 51$ grid

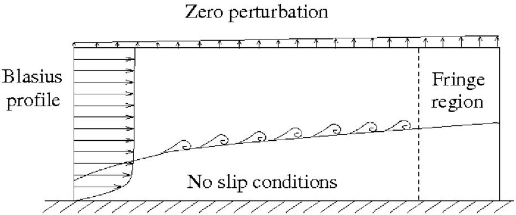

Power iterations for the optimization

Lagrange multipliers method

The Objective function is the kinetic energy integrated in the whole domain:

$$\mathcal{J} = E(t) = \frac{1}{2}\int_0^{L_x}\int_0^{L_y}\int_{-Z}^{Z}\left(u^2+v^2+w^2\right)\,dxdydz. \tag{4}$$

Constraint: NS equations $\longrightarrow$ First variation of the augmented fuctional set to zero $\longrightarrow$ adjoint equations plus compatibility and optimality conditions

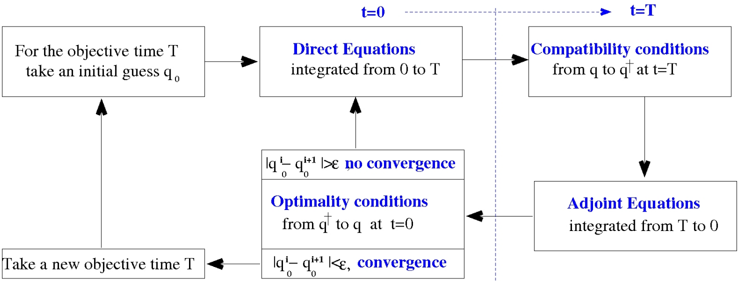

Global instability model

The instantaneous variables $\mathbf{q} = (u, v, p)^T$ are considered as a superposition of the base flow and of the perturbation $\tilde{\mathbf{q}} = (\tilde{u}, \tilde{v}, \tilde{p})^T$.

Decomposition of the perturbation on a basis of N temporal modes:

$$\tilde{\mathbf{q}}(x, y, z, t) = \sum_{k=1}^{N} \kappa_k^0 \, \hat{\mathbf{q}}_k(x, y) \exp\left(-i(\omega_k t + \beta z)\right),$$

where $\hat{\mathbf{q}}_k$ are the eigenvectors, ω_k the eigenvalues, κ_k^0 their initial amplitude.

Substituting in the NS eq. and linearizing lead to the eigenvalue problem:

$$(\mathbf{A} - i\omega_k \mathbf{B}) \, \hat{\mathbf{q}}_k = \mathbf{0}, \quad k = 1, \ldots, N. \tag{5}$$

discretized with a Chebyshev/Chebyshev spectral method employing $N = 850$ modes on a 270×50 grid, and solved by a shift and invert Arnoldi algorithm.

Maximum energy gain at time t over all possible initial conditions $\mathbf{u}_0$

$$G(t) = \max_{\mathbf{u}_0 \neq 0} \frac{E(t)}{E(0)} = ||\mathbf{F} \exp(-it\mathbf{\Lambda})\mathbf{F}^{-1}||_2^2 \tag{6}$$

where $\mathbf{\Lambda}_{k,l} = \delta_{k,l}\omega_k$ and $\mathbf{F}$ is the Cholesky factor of the energy matrix $\mathbf{M}$ of components $M_{ij} = \int\int (\hat{u}_i^* \hat{u}_j + \hat{v}_i^* \hat{v}_j + \hat{w}_i^* \hat{w}_j) \, dxdy, \; i, j = 1, \ldots, N$

Why should *optimals* (= right singular vectors) be relevant at all ? They are not !

The propagator $\mathbf{P}$ of the initial condition $\tilde{\mathbf{q}}_0$ turns the initial state into a final state $\tilde{\mathbf{q}}_T$.

Singular Value Decomposition:

$$\mathbf{P} = \mathbf{L}\boldsymbol{\Sigma}\mathbf{R}^*,$$

with $\mathbf{L}$ and $\mathbf{R}$ unitary matrices, $\boldsymbol{\Sigma}$ diagonal matrix of singular values.

Suppose that the initial state could be expressed as a (hopefully) balanced expansion of the right singular vectors:

$$\tilde{\mathbf{q}}_0 = \mathbf{R}\mathbf{a} \tag{7}$$

with $\mathbf{a}$ *vector of coefficients,*

then the output is a combination of left singular values:

$$\tilde{\mathbf{q}}_T = \mathbf{L}\boldsymbol{\Sigma}\mathbf{R}^*\mathbf{R}\mathbf{a} = \mathbf{L}\left[\boldsymbol{\Sigma}\mathbf{a}\right]. \tag{8}$$

Depending on the properties of the spectrum of singular values, the left singular vector associated to the largest singular value may dominate the dynamics at $t = T$.

Linear Results

Optimal energy gain

- **Optimal energy gain** for $Re = 610$: $G(t_{max}) = 736$ at $t_{max} = 247$, larger than the value found by a local approach at the same Re.
- **Convergence**: the optimization method reaches in 20 iterations a level of convergence of about $e = 10^{-4}$, in 80 it converges up to $e = 10^{-5}$ ($e = (E^{(n)} - E^{(n-1)})/E^{(n)}$).

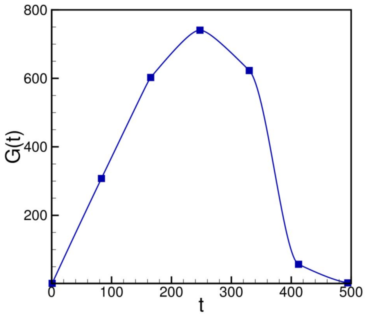

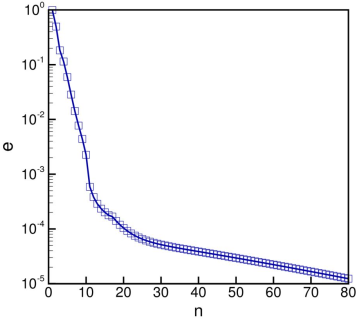

Optimal perturbation in the plane y-z

The optimal perturbation is characterized in the plane $y - z$ by a pair of counter-rotating vortex, like the local optimal with $\alpha = 0$ (Farrell 1988).

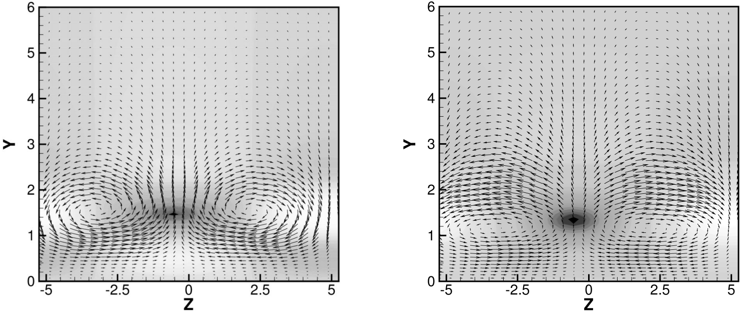

Figure: Optimal perturbation at $t = 0$ and $t = t_{max}$ for $Re = 610$. Vectors represent the wall-normal and spanwise velocity components, shades of grey are relative to the streamwise velocity.

Optimal perturbation at $t = 0$

- **Local optimization**: optimal perturbation for $\alpha = 0$
- **Global optimization**: optimal perturbation composed by upstream-elongated packets, tilted upstream, **modulated in the x direction** $(\alpha \neq 0)$

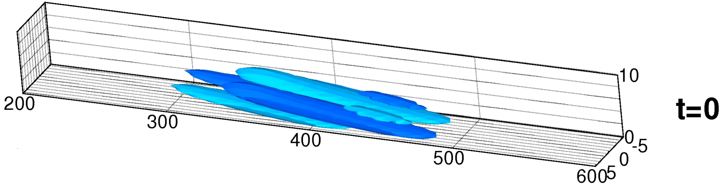

Figure: Iso-surfaces of the streamwise component of the optimal perturbation at $t = 0$.

What does the optimal perturbation turn into?

- **Orr mechanism**: tilts the perturbation in the mean flow direction.
- **Lift-up mechanism**: amplifies the streamwise perturbation.
- **At optimal time**: streaky structures alternated in the x direction.

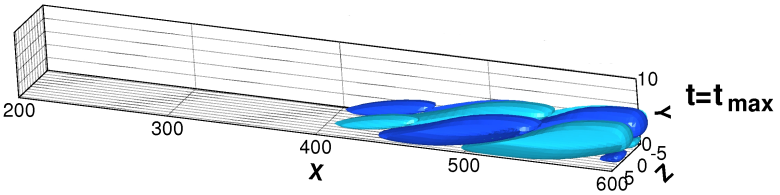

Figure: Iso-surfaces of the streamwise component of the optimal perturbation at $t = t_{max}$.

The streamwise modulation

Dependence on the streamwise domain length

Optimizations with streamwise domain lengths $L_x = 400, 800, 1200$

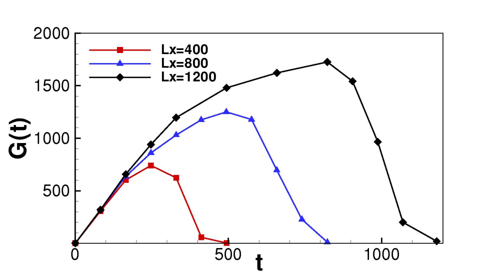

- G_{max} increases due to a combined effect of the Orr mechanism and of the spatial non-parallel amplification
- T_{max} increases linearly due to base flow advection ($t \propto L_x/U_\infty$)

The optimal perturbations plotted on the normalized coordinates $\eta = y\sqrt{Re/x}$, $\bar{x} = xL_{x_1}/L_x$ present **a similar longitudinal extent, inclination, and modulation.**

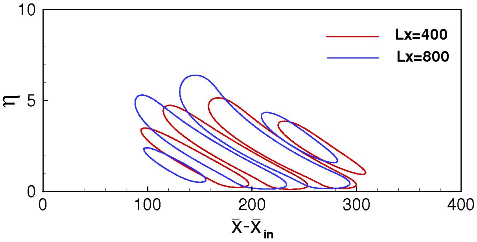

Streamwise characteristic wavenumber (dependence on L_x)

The most amplified wavenumber of the optimal perturbation, α_c, is computed by spatial Fourier transform for different target times and L_x.

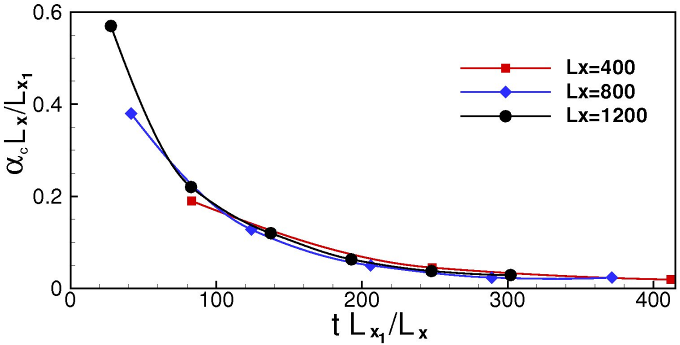

- The normalized modulation of the perturbation is approximately **invariant** with respect to the value of L_x used in the optimization.
- α_c is rather high at small times and decreases with time towards an asymptotic value.

Dependence on Re

- The optimal perturbation is computed at $Re = 610, 300, 150$.
- At all Re the optimal perturbation is modulated in the x-direction.
- The streamwise modulation of the perturbation in normalized coordinates is found to vary

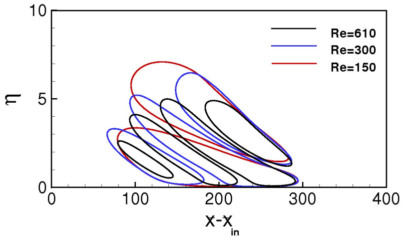

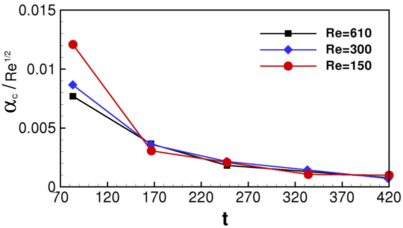

The characteristic wavenumber is found to increase approximately with the square root of Re $\rightarrow$ the curves of α_c normalized with $\sqrt{Re}$ collapse onto one for sufficiently large times

Scaling law for α_c

The scaling law for the characteristic streamwise wavenumber:

$$\alpha_c \propto \frac{\sqrt{Re}}{L_x} \tag{9}$$

- provides the variation of the optimal $x-$modulation with the independent parameters of the optimization, L_x and Re.
- allows to recover the classical result on the optimal growth in a parallel boundary layer, since $\alpha_c \rightarrow 0$ for $L_x \rightarrow \infty$.

The origin of such a modulation is investigated: could it be related to (a superposition of) local single-wavenumber optimals?

A three-dimensional perturbation is reconstructed as a superposition of local optimals ($\alpha = 0$) and suboptimals ($\alpha \neq 0$) :

$$\mathbf{q}(x, y, z) = \sum_{j=1}^{n} \kappa_j \, \bar{\mathbf{q}}_j(y) \exp\left(i\beta z - i\alpha_j x\right), \tag{10}$$

where $\bar{q}_j(y)$ is the result of the local optimization in Corbett & Bottaro 2000 for a given α, at the energy κ_j.

Local approximation and streamwise modulation

Local approximation

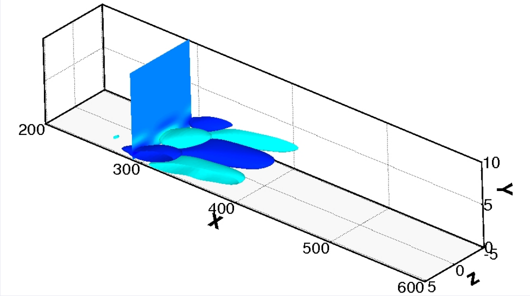

Superposition of local optimals and suboptimals at different α $\longrightarrow$ the global optimal perturbation is qualitatively recovered

The characteristic streamwise wave number α_c *converges with time to a value different from zero* $\longrightarrow$ well predicted by the superposition of local optimals

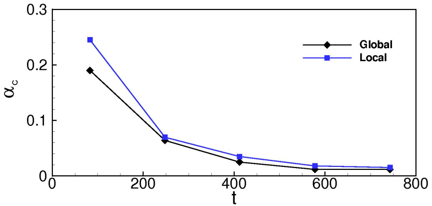

The spanwise modulation and the *near-optimal* perturbation

Effect of the spanwise direction

Optimal energy gain for different spanwise domain lengths, L_z:

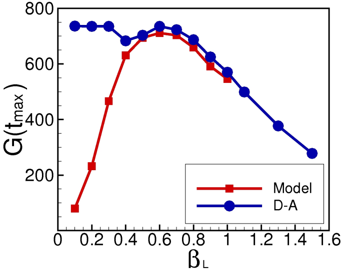

- **Global model**$\rightarrow$ β is fixed $\rightarrow$ well defined peak for $\beta = 0.6$
- **Direct-adjoint**$\rightarrow$ Just the minimum β is fixed, $\beta_L = 2\pi/L_z$ $\rightarrow$ for low β_L (large L_z) the dynamics matches the optimal one (more than one wave appears at small β)

- *The optimal perturbation is single-wavenumber and extended in z, because the problem is homogeneous in z*
- **A realistic perturbation is localized in the spanwise direction and composed by a spectrum of β.**

The global near-optimal perturbation

We look for a *near-optimal* perturbation:

- localized in the spanwise direction
- composed by a spectrum of β
- reaching a *near-optimal* value of $G(t)$

Thus, we follow the procedure below.

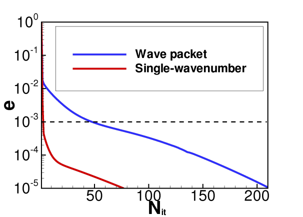

1. *We build an artificially localized wave packet by multiplying the optimal single-wavenumber perturbation times an envelope of the form* $\exp(-z^2)$
2. *We initialize the optimization with such artificial wave packet*
3. *We stop the iterations at* $e = 10^{-3}$, *when the largest residual adjustments of the solution occur in the spanwise direction*
4. *Since the problem is self-adjoint in* z, *the influence of the spanwise shape of the perturbation on the energy gain is weak with respect to the streamwise and wall-normal ones*

Near-optimal wavepacket

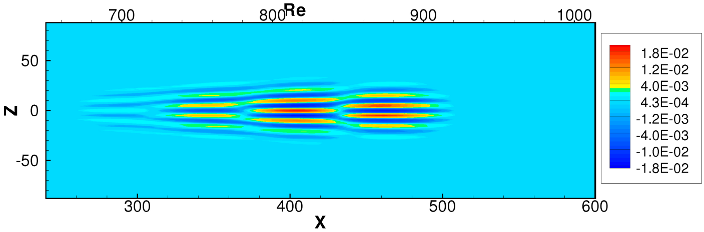

Figure: Streamwise near-optimal perturbation at $t = 0$, $y = 1$.

Thus, we obtain a *near-optimal* perturbation

- localized in the spanwise direction
- composed by a spectrum of β
- **reaching 99% of the value of $G(t_{max})$!**

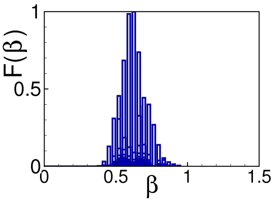

Non-Linear Results

Transition energy levels (global vs local optimals)

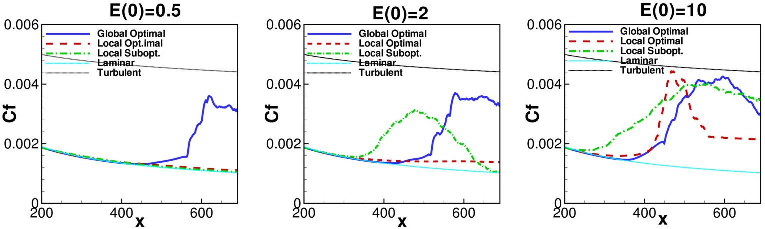

Figure: Mean skin friction factor of the considered flow perturbed with global, local, and sub-optimal disturbances, for from left to right $E_0 = 0.5$, $E_0 = 2$ and $E_0 = 10$.

What perturbation is most effective in inducing transition?

- **Local optimal at** $\alpha = 0$: transition for $E_0 = 10$.
- **Local suboptimal at** $\alpha \neq 0$: transition for $E_0 = 2$ (Biau et al. 2008).
- **Global three-dimensional optimal**: transition for $E_0 = 0.1$.
- **The global optimal perturbation is the most effective in inducing transition, followed by the suboptimal one.**

Transition induced by the near-optimal perturbation

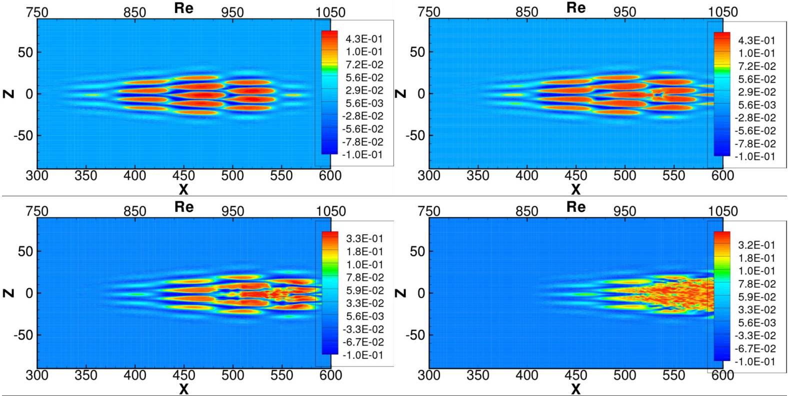

Streamwise velocity contours at $y = 1$ and $E_0 = 0.5$ at four times:

- $T = 160$: saturation and presence of spanwise subharmonics.
- $T = 220$: *kinks* at the front of the most amplified streak.
- $T = 250$: spreading out of the turbulence to the confining streaks.
- $T = 330$: presence of a **turbulent spot**

Transition to a turbulent spot

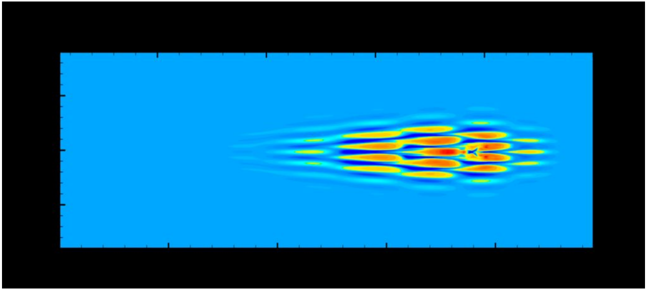

Streaks breakdown

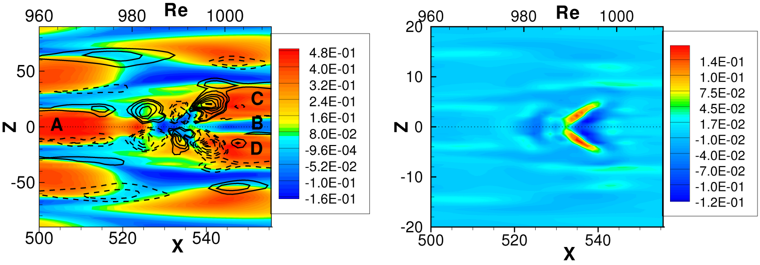

Figure: Streamwise (a) and wall-normal (b) perturbation at $T = 220$. The solid and dashed lines represent positive and negative spanwise velocities.

Quasi-sinuous or quasi-varicose oscillations of the streaks?

- Both quasi-sinuous (C,D) and quasi-varicose (A,B) oscillations are recovered, due to the staggered arrangement of the streaks
- **Four streaks (A,B,C,D) break down at the same time, explaining the efficiency of the perturbations in provoking transition.**

Vortical structures

- *Recently, Wu & Moin have given evidence of the presence of hairpin vortices in transitional boundary-layer flows*
- We visualize the vortical structures by the Q-criterion
- **An hairpin vortex** is identified in the interaction zone of the streaks A,B,C,D, preceded upstream by a pair of **quasi-streamwise** vortices

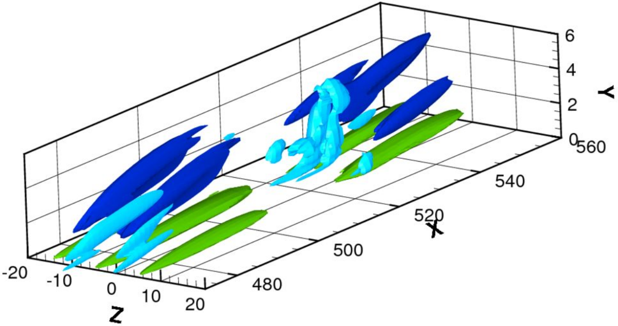

Figure: Iso-surfaces of negative (blue) and positive (green) streamwise perturbations, and Q-criterion surfaces (light blue).

The hairpin vortices formation (1)

- At $t = 145$, two **quasi-streamwise vortices** are present on the flanks of the low-speed streak, increasing their size on the wall-normal direction. An **inclined shear layer** is induced by the front interaction of the low- and high-speed streaks

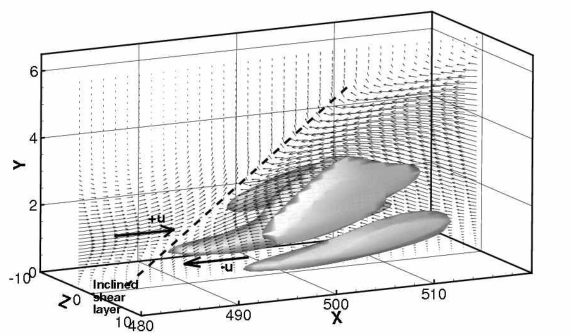

Figure: Iso-surfaces of the Q criterion and u, v, w vectors on the $x - y$ plane at $z = 0$ at $t = 145$.

The hairpin vortices formation (2)

- At $t = 165$: non-linear effects allow the formation of a vortical region at the edge of the inclined shear layer connecting the two quasi-streamwise vortices, thus forming the head of the hairpin.

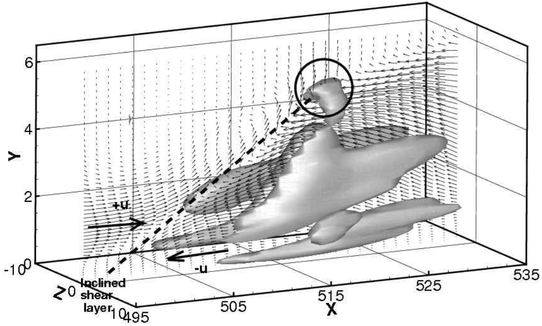

Figure: Iso-surfaces of the Q criterion and u, v, w vectors on the $x - y$ plane at $z = 0$ at $t = 165$.

The hairpin vortices formation (3)

- At $t = 180$: the primary hairpin head is lifted from the wall, and a second arch vortex appears upstream of the first along the inclined zone of interaction of the low and high-speed streaks. A similar dynamics is observed for turbulent boudary layers (Adrian 2007),

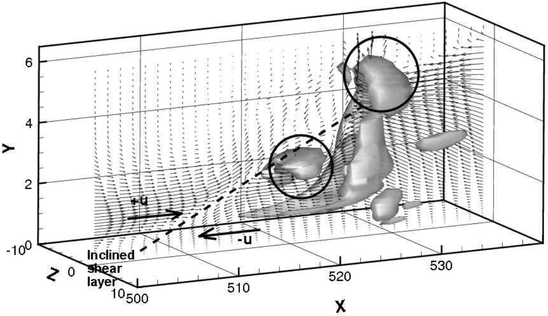

Figure: Iso-surfaces of the Q criterion and u, v, w vectors on the $x-y$ plane at $z=0$ at $t=180$.

The hairpin vortices formation (4)

- At $t = 190$: the first hairpin vortex increases in size, breaking up into smaller coherent patches of vorticity, although remnants of the original structure are still visible.

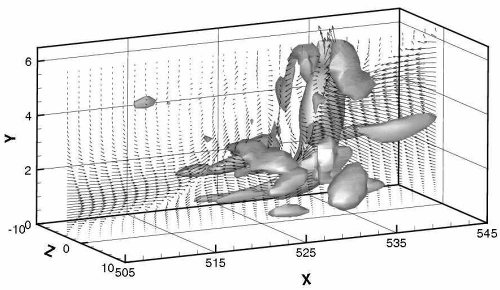

Figure: Iso-surfaces of the Q criterion and u, v, w vectors on the $x - y$ plane at $z = 0$ at $t = 190$.

Such a transition scenario connects two opposite views of transition, that grounded on transient growth and secondary instability of the streaks (Schoppa & Hussain, 2002), and the other based on vortex regeneration (Adrian 2007).

Conclusions and perspectives

1. The global optimal perturbation is characterized non-zero streamwise wavenumber.
2. It is **more effective in inducing transition** than a local suboptimal or a local optimal one.
3. A *near-optimal perturbation*, localized also in the spanwise direction, transitions in a **turbulent spot**.
4. **Quasi-sinous and quasi-varicous streaks oscillations** are recovered due to the staggered arrangement of the streaks.
5. **An hairpin vortex** is identified in the interaction zones of such streaks, induced by the front interaction of the low- and high-speed streaks.
6. ***A viable path to transition is presented, connecting the transition scenario based on transient growth (Schoppa & Hussain 2002) and that based on vortex regeneration (Adrian 2007).***